IEEE Access
Multidisciplinary | Rapid Review | Open Access Journal

Received 23 August 2023, accepted 23 October 2023, date of publication 26 October 2023, date of current version 3 November 2023.

Digital Object Identifier 10.1109/ACCESS.2023.3327815

RESEARCH ARTICLE

A Human-Like Free-Lane-Change Trajectory Planning and Control Method With Data-Based Behavior Decision

LIANG CHU[1], (Member, IEEE), JIAWEI WANG[1], ZHUO CAO[1], YAO ZHANG[1], AND CHONG GUO[1,2]

[1]College of Automotive Engineering, Jilin University, Changchun 130022, China
[2]Changsha Automobile Innovation Research Institute, Changsha 410005, China

Corresponding author: Chong Guo (guochong@mail.jlu.edu.cn)

ABSTRACT Free lane change (FLC) is an important research direction of intelligent driving vehicles. In this paper, a lane change decision model based on deep learning is established with ego and adjacent lane risk and properties of environmental vehicles. A long short-term memory neural network that can be associated with time series characteristics is used to model the lane change process based on analysis of factors affecting the lane change decision. The result of decision-making model training shows that the recognition accuracy of lane change and lane keeping decision reaches more than 92%. Then, a human-like FLC trajectory is planned based on polynomial curve, a quintic polynomial trajectory cluster based on preview distance is generated according to driving conditions, and the optimal FLC trajectory is selected by optimizing an objective function. The model predictive control method is used to dynamically control the vehicle to follow the trajectory. Finally, the lane change decision, trajectory planning, and tracking control model are built in simulation environment, and the control of vehicle dynamics model verifies the integrity and feasibility of free lane change function.

INDEX TERMS Autonomous driving, lane change decision, trajectory planning, tracking control.

I. INTRODUCTION

The development of automobiles has brought great convenience to human travel, and intelligent driving can help people better improve driving safety and traffic efficiency. In the studies of intelligent driving, autonomous lane change is an important part. An effective way to make lane change decision ensures high driving safety and fast driving efficiency at the same time. After autonomous vehicle decides to change lane, it is also necessary to provide the correct lane change timing and reasonable lane change trajectory according to the current surrounding environment so as to control the vehicle state in real time during lane change process to follow the expected driving trajectory.

Changing lanes too frequently or ignoring the surrounding vehicles to forcibly change lanes can lead to traffic congestion and dangerous driving conditions, so it is necessary to reasonably formulate a strategy for changing lanes. In addition, the proper design of motion planner and trajectory tracker is also an important guarantee for enabling vehicle to generate and follow suitable lane change trajectory. There has been a great deal of research in lane change decision making, trajectory planning and tracking control. In terms of lane change decision, rule-based methods [1], [2], [3], [4] are used to calculate the driver's dissatisfaction with the current lane based on factors such as the distance between ego vehicle and front vehicle, and consider the trade-off between safety and lane change benefits to make the choice of whether to change lanes. Based on the classification method of machine learning, support vector machine [5], hidden Markov model [6], and BP neural network [7], [8] are used to depend the driving conditions of ego vehicles to determine following front vehicle or timing of lane change. When ego vehicle is running on open roads, changes in other traffic participants

The associate editor coordinating the review of this manuscript and approving it for publication was Jason Gu.

will affect the behavior of ego vehicle, so lane change decision needs to consider the interaction of surrounding environmental factors. Game theory [9], [10], and adversarial training [11] are used to establish the reward function of different traffic participants to design the lane change-avoidance decision model of autonomous vehicle in intelligent driving environment. In addition, with the enrichment of intelligent driving datasets, data models based on deep learning and reinforcement learning have been proposed in large numbers. Based on deep learning networks such as convolutional network [12], [13], and deep confidence network [14], Lane change decision models are established based on reinforcement learning network [15], [16]. Inputs of these data-driven models are location, velocity, acceleration, and relative information of ego vehicle and environmental traffic participants. Compared with traditional theoretical model-based methods, since the inputs are all real-world traffic data, the output lane change decision can be largely similar to real drivers. In terms of trajectory planning of vehicles, the trajectory shapes mainly include trigonometric curves [17], B-spline curves [18], numerical optimization trajectories [19], and polynomial curves [20], etc. Among them, polynomial curve method is currently the most widely used lane change trajectory planning algorithm because it can fully consider the dynamic and kinematic characteristics of vehicle, and can be used in complex driving environments with moving obstacles, and even for some extreme driving conditions. In terms of trajectory tracking control, proposed methods include optimal control linear secondary regulator [21], lateral acceleration feedback adaptive fuzzy PID controller [22], and adaptive synovial membrane controller [23], etc. The control effect has been well verified.

The above-mentioned research on lane change fully integrates lane change decision with environmental information and achieves good results. However, the input of the proposed learning model rarely has the design of target lane risk in advance, and the particle model is mostly adopted when extracting vehicle driving data input by the learning model and ignores vehicle shape and size, and it is rare to make joint lane change decisions and subsequent trajectory planning and tracking research. In order to consider the risks of lane keeping and left-right changing in advance, and control the specific behavior of vehicle after making decision, this paper proposes a data-driven lane change decision model based on lane risk, then determines and optimizes the lane change trajectory, and designs the trajectory tracking controller to ensure that the vehicle can realize the lane change behavior according to the planned trajectory. The lane change decision uses the Long Short-Term Memory (LSTM) model to determine whether lane change should be carried out in different driving scenarios by encoding the decision result of lane change, environmental vehicles information and the risk of lane changing. Based on the generated lane change decision, a human-like lane change trajectory planner based on preview model and quintic polynomial is developed, which provides a reference trajectory for lane change behavior. By setting different preview positions, lane change trajectory clusters are generated, and the optimal lane change trajectory is determined by combining safety and comfort indicators. Then, a Model Predictive Control (MPC) method is designed to track the lane change trajectory generated in different driving scenarios.

The contributions of this paper are divided into the following three points:

1) A deep learning lane change decision method considering different lane risks is proposed, and characteristic variables such as lane risk and environmental vehicles motion information are introduced at the input layer, which adds the lane risk term in the learning process and is conducive to increasing the dimension of lane change decision consideration.

2) Compared with the conventional method of calculating characteristic variables using vehicles as particles, the shape and size information of environmental vehicles is introduced through risk terms, and the occupancy of lanes by vehicles of different types and sizes can be taken into account, and the scene understanding of autonomous vehicles can be enhanced.

3) According to decision-making results, a lane change trajectory planning and tracking control model is built, and based on Carmaker's vehicle dynamics model and sensor perception of environmental vehicles, the co-simulation with SIMULINK verifies the proposed model.

The rest of this paper is organized as follows: section II introduces the establishment and training process of LSTM network for lane change decision. Section III provides a lane change trajectory planner based on preview model and quintic polynomial and a trajectory tracking controller based on MPC. Section IV provides co-simulation verification results based on Carmaker and SIMULINK. Finally, section V summarizes this paper and proposes future research directions.

II. DATA-BASED FREE LANE CHANGE DECISION

In the lane change decision stage and the process of lane changing, it is necessary to comprehensively measure the vehicles in front and rear of the original lane and adjacent lanes, but also consider the influence of ego vehicle behavior on the traffic flow. The vehicle's lane change behavior is divided into two types: forced lane change and free lane change, the former refers to the change of lane that driver must make in order to reach the destination due to regulatory restrictions or changes in road conditions. The latter is the behavior of changing lanes when vehicle can reach the destination smoothly regardless of whether it changes lanes or not. For autonomous vehicles, forced lane change behavior is necessary and does not need to consider lane change decisions; while the free lane change decision leads to potential driving efficiency gains and better safety. At present, there are many data sets that record vehicles following or changing lanes in traffic flow, and the conditions for vehicles to choose lane changing can be determined in a data-driven way based on past state information of vehicles in traffic flow

and driving risks of different lanes. Therefore, this section focuses on decision making process for free lane changes of vehicle.

A. FREE LANE CHANGE DECISION ANALYSIS

The decision of free lane change is a process of comprehensively considering the state of vehicles around ego vehicle to determine whether it is necessary to make a lane change decision, and first need to identify the vehicles involved in the decision process and their states. Most of the reasons for free lane change are that the current lane is slower to travel, i.e., vehicle in front of ego lane is slow compared to the speed limit or closer to ego vehicle. While the lateral offset and lateral velocity of front vehicle will affect the choice of lane change direction. Therefore, the current lane speed limit and the lateral and longitudinal movement of front vehicle are important lane change decision factors. If rear vehicle in current lane has the intention to change lanes in the same direction, ego vehicle might abandon the original lane change decision, so the position and speed information of the rear vehicle in current lane are used as factors affecting the current vehicle lane change decision. The adjacent lanes on the left and right sides are potential lane change targets, so driving data of vehicles in front and rear on the adjacent lanes are required. Therefore, it is necessary to use the micro-traffic environment consisting of six vehicles in front and rear the current lane and the adjacent lanes as the decision space for lane change, as shown in Figure 1. Where ego means ego vehicle, egoF and egoR are front and rear vehicle in current lane, LF and LR are front and rear vehicle in left lane, RF and RR are front and rear vehicle in right lane, the subscript with dx means the distance between ego vehicle and the vehicle which subscript indicates. The factors that affect lane change are shown in Table 1.

The factors that affect lane change decision are mainly the surrounding vehicles state and the congestion of ego lane. Based on the influencing factors in Table 1, ego vehicle state is marked as $\Omega_{ego} = [v_{ego}, a_{ego}, v_{limit}]$, front vehicle state is marked as $\Omega_{egoF} = [d_{xegoF}, d_{yegoF}, v_{x_{egoF}}, v_{yegoF}]$, rear vehicle state is marked as $\Omega_{egoR} = [d_{xegoR}, d_{yegoR}, v_{xegoR}, v_{yegoR}]$, left front vehicle state is marked as $\Omega_{LF} = [d_{xLF}, d_{yLF}, v_{xLF}, v_{yLF}]$, left rear vehicle state is marked as $\Omega_{LR} = [d_{xLR}, d_{yLR}, v_{xLR}, v_{yLR}]$, right front vehicle state is marked as $\Omega_{RF} = [d_{xRF}, d_{yRF}, v_{xRF}, v_{yRF}]$, right rear vehicle state is marked as $\Omega_{RR} = [d_{xRR}, d_{yRR}, v_{xRR}, v_{yRR}]$. From the perspective of traffic flow, the state of surrounding vehicles in a certain time period has an impact on ego vehicle's decision to change lanes. Therefore, this paper argues that lane change decision is determined by the sequence of ego vehicle and environmental vehicle states over a time period and the traffic risks of ego and adjacent lanes.

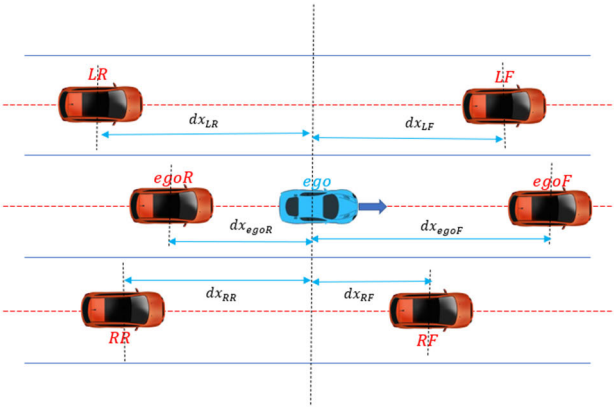

FIGURE 1. Micro-traffic environment for lane change decision, ego vehicle is in blue, while environmental vehicles are in red.

TABLE 1. Factors influencing lane change decision.

Factor	Quantity	Factor	Quantity
v_{ego}	Ego vehicle velocity (m/s)	$v_{y_{LF}}$	Left front vehicle lateral velocity (m/s)
a_{ego}	Ego vehicle accel (m/s^2)	$d_{x_{LR}}$	Left rear vehicle longitudinal distance (m)
v_{limit}	Lane velocity limit (m/s)	$d_{y_{LR}}$	Left rear vehicle lateral distance (m)
$d_{x_{egoF}}$	Front vehicle longitudinal distance (m)	$v_{x_{LR}}$	Left rear vehicle longitudinal velocity (m/s)
d_{yegoF}	Front vehicle lateral distance (m)	$v_{y_{LR}}$	Left rear vehicle lateral velocity (m/s)
$v_{x_{egoF}}$	Front vehicle longitudinal velocity (m/s)	$d_{x_{RF}}$	Right front vehicle longitudinal distance (m)
v_{yegoF}	Front vehicle lateral velocity (m/s)	$d_{y_{RF}}$	Right front vehicle lateral distance (m)
$d_{x_{egoR}}$	Rear vehicle longitudinal distance (m)	$v_{x_{RF}}$	Right front vehicle longitudinal velocity (m/s)
d_{yegoR}	Rear vehicle lateral distance (m)	$v_{y_{RF}}$	Right front vehicle lateral velocity (m/s)
$v_{x_{egoR}}$	Rear vehicle longitudinal velocity (m/s)	$d_{x_{RR}}$	Right rear vehicle longitudinal distance (m)
v_{yegoR}	Rear vehicle lateral velocity (m/s)	$d_{y_{RR}}$	Right rear vehicle lateral distance (m)
$d_{x_{LF}}$	Left front vehicle longitudinal distance (m)	$v_{x_{RR}}$	Right rear vehicle longitudinal velocity (m/s)
$d_{y_{LF}}$	Left front vehicle lateral distance (m)	$v_{y_{RR}}$	Right rear vehicle lateral velocity (m/s)
$v_{x_{LF}}$	Left front vehicle longitudinal velocity (m/s)		

B. LANE CHANGE SAMPLE PROCESSING

The NGSIM (Next Generation Simulation) dataset is selected, which records the numbers of different lanes on a section of highway and the dimensions, lateral and longitudinal coordinates, speed and acceleration information

of vehicles traveling on these lanes, recording frequency is 10 Hz. In this paper, the lateral and longitudinal velocity and acceleration of vehicles with different IDs are calculated with dimensions and position information based on vehicle kinematics, and the lane risk is calculated according to the risk analysis method.

The longitudinal velocity is:

$$v_{x_t} = \frac{Pos_{x_t+1} - Pos_{x_t-1}}{\Delta t} \tag{1}$$

where v_{x_t} is the velocity of vehicle in x direction at time t; Pos_{x_t+1} is the coordinate of vehicle in the x direction at time $t+1$; Pos_{x_t-1} is the coordinate of vehicle in x direction at time $t-1$; Δt is the time difference between time $t+1$ and time $t-1$.

The lateral velocity is:

$$v_{y_t} = \frac{Pos_{y_t+1} - Pos_{y_t-1}}{\Delta t} \tag{2}$$

where v_{y_t} is the velocity of vehicle in y direction at time t; Pos_{y_t+1} is the coordinate of vehicle in the y direction at time $t+1$; Pos_{y_t-1} is the coordinate of vehicle in y direction at time $t-1$; Δt is the time difference between time $t+1$ and time $t-1$.

The acceleration of ego vehicle is:

$$a_{ego_t} = \frac{v_{ego_t+1} - v_{ego_t-1}}{\Delta t} \tag{3}$$

where a_{ego_t} is the acceleration of ego vehicle at time t; v_{ego_t+1} is the velocity of ego vehicle at time $t+1$; v_{ego_t-1} is the velocity of ego vehicle at time $t-1$; Δt is the time difference between time $t+1$ and time $t-1$.

Lane risk consists of static risk and dynamic risk calculated using a two-dimensional Gaussian function. The static risk is

$$U_{sta} = exp\left(-\left(\left(\frac{(x-x_{obs})^2}{L_{obs}^2}\right)^2 + \left(\frac{(y-y_{obs})^2}{W_{obs}^2}\right)^2\right)\right) \tag{4}$$

e dynamic risk is

$$U_{dyn} = \frac{exp\left(-\left(\left(\frac{(x-x_{obs})^2}{6|v_{obsx}-v_{egox}|}\right)^2 + \left(\frac{(y-y_{obs})^2}{6|v_{obsy}-v_{egoy}|}\right)^2\right)\right)}{1 + exp\left(-rel_v\left(x - x_{obs} - 0.9L_{obs}\cdot rel_v\right)\right)} \tag{5}$$

$$rel_v = \begin{cases} 1, v_{obsx} \geq v_{egox} \\ -1, v_{obsx} < v_{egox} \end{cases} \tag{6}$$

The total risk is

$$U = U_{sta} + U_{dyn} \tag{7}$$

where (x, y) is the coordinates of ego vehicle, (x_{obs}, y_{obs}) is the center point coordinate of obstacle vehicle, (L_{obs}, W_{obs}) is length and width of obstacle vehicle, v_{obsx} is longitudinal velocity of obstacle vehicle, v_{egox} is longitudinal velocity of ego vehicle, rel_v is a function that describes the direction of movement with obstacles and ego vehicle relative to each other. If there are multiple obstacle vehicles on a lane, the lane risk is the summation of each obstacle vehicle.

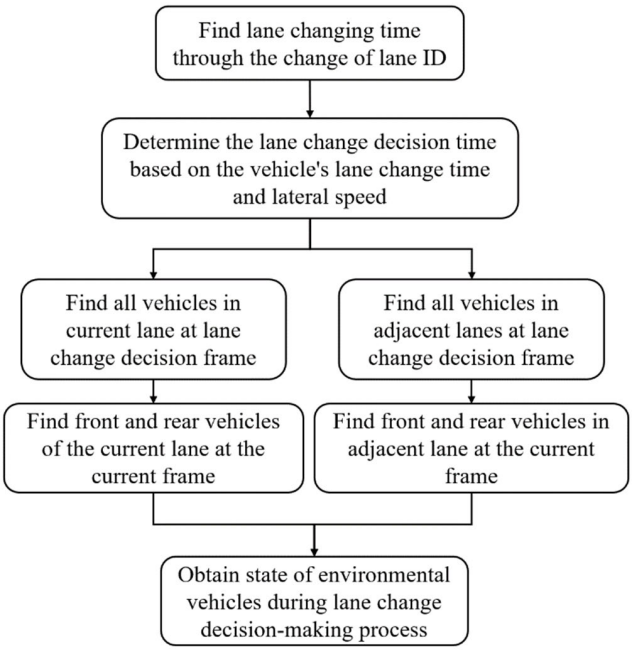

FIGURE 2. Data extraction process.

This paper uses lateral velocity to judge the start point of lane change, and when the vehicle lateral velocity is greater than 0.1m/s, it is considered to start changing lanes, so the need is to filter out the position of each vehicle's lateral velocity greater than 0.1m/s or less than -0.1m/s for the first time as the position where vehicle begins to change lane left or right. According to the conclusion of [24], there is a buffer time of 0.5 seconds between decision and execution of lane change, which is called time window. Therefore, the time corresponding to the start position of lane change is pushed forward by 0.5 seconds as the moment of the lane change decision. When the lane ID of vehicle changes, record this moment as the lane change time. Then look forward to the time when the last lateral velocity is between ±0.1m/s as the start moment of lane change, and push forward 0.5 seconds as the moment when the lane change decision is generated. Next, data on surrounding vehicles needs to be extracted, as shown in Figure 2.

The data processing of lane change decisions needs to take into account the positive and negative samples of lane change decisions, where the positive sample is to make the left lane change (LLC) decision and the right lane change (RLC) decision, and the negative sample is to make the lane keeping (LK) decision. The reason for LK may be that the current lane driving condition is better and there is no need to change lanes or because the traffic conditions in the adjacent lane are similar to the current lane, and neither of them meets the driver's expectations. The former is more likely to correspond

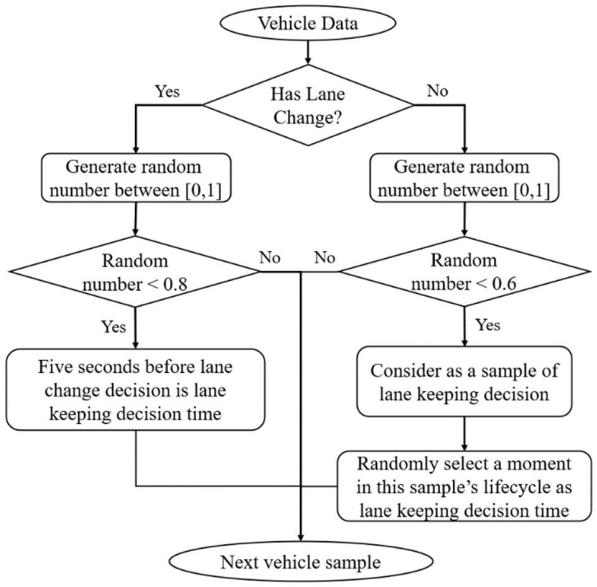

FIGURE 3. Decision sample selecting.

to vehicles that have never changed lanes during the entire driving process of road section. LK performed by a vehicle that changes lanes before the driver makes a lane change decision is more likely to correspond to the latter. Therefore, all conditions within 5 seconds before the time of lane change decision are used as a LK decision sample that cannot meet the driver's expectations. In addition, a sample of LK from vehicles that never changed lanes is randomly retained. Data filtering is done using a random function, while the state of surrounding vehicles for the selected LK sample is obtained using the same method as screening the lane change sample, as shown in Figure 3.

For the filtered lane change samples, the following processing is required: (i) delete the ramp change data; (ii) delete samples of average velocity below 3m/s; (iii) Delete continuous lane change samples. After randomly shuffling the lane change data and lane keeping data, 80% of all data samples were selected as training samples; The remaining 20% were used as test samples. In order to ensure data consistency, the data is dedimensionalized and the maximum and minimum values are limited and normalized. Limit the longitudinal distance to -150m to 150m and velocity to 0-25m/s. Attributes of longitudinal velocity, lateral velocity, longitudinal relative distance, lateral relative distance, and longitudinal acceleration are extracted, and all the data of same attribute are fused together for preprocessing. The distance between traffic participants and ego vehicle represents former's left and right orientation information to the letter. The acceleration of the vehicle represents the physical properties of the acceleration and deceleration state of the vehicle. Normalize the positive and negative distance and acceleration values between [0, 1] and [−1,0] with 0 as the dividing line, respectively.

$$\begin{cases} x_{std} = x/x_{max}, x \geq 0 \\ x_{std} = -x/x_{min}, x < 0 \end{cases} \tag{8}$$

where x represents the lateral and longitudinal distance or longitudinal acceleration, x_{max}, x_{min} represents the maximum and minimum values of the lateral and longitudinal distance or longitudinal acceleration, and x_{std} represents the normalized result.

Since the vehicle velocity is positive, velocity is directly normalized to [−1,1]:

$$x_{std} = -1 + 2\left(\frac{x - x_{min}}{x_{max} - x_{min}}\right) \tag{9}$$

where x represents the vehicle velocity, x_{max}, x_{min} represents the maximum and minimum vehicle velocity, and x_{std} represents the normalized result.

The risk U_L of left lane, the risk U_E of ego lane, and the risk U_R of right lane are calculated and normalized.

$$(U_L, U_E, U_R) = \frac{(U_L, U_E, U_R)}{U_L + U_E + U_R} \tag{10}$$

C. LANE CHANGE DECISION MODEL

The Long Short-Term Memory (LSTM) neural network is selected, and the input layer nodes include the 30 attributes involved in the lane change decision proposed in Section III-A and the risk of ego lane and adjacent two lanes. The reason why acceleration less considered in model input is that LSTM network has memory function, once the velocity term is entered, its first derivative (i.e., acceleration) will appear in the network. The LSTM layer of the lane change decision model should have three output nodes, activation function selects softmax.

$$S_i = \frac{e^{y_i}}{\sum_j e^{y_j}} \tag{11}$$

where S_i is the output of i-th node, y_i is the input of i-th node, and $\sum_j e^{y_j}$ means the exponential sum of all node inputs. A layer of softmax function is used to produce three output nodes, the values of which are all between [0 1], and the node value is probability of choosing the corresponding lane. The output of the lane change decision corresponds to the three dimensions of left lane change, lane keep and right lane change, the decision result should be [LLC LK RLC]. The hidden layer of lane change decision model is dominated by LSTM neural network units. After the LSTM layer, a fully connected layer with three output nodes is set. In order to prevent the model from overfitting, add a dropout layer after each hidden layer, and the probability will temporarily discard some neural units from the network, setting the dropout probability to 0.5. The loss function takes cross-entropy loss, while for classification problems, the loss value for each output is calculated as

$$L = -\sum_{c=1}^{3} y_c \log p_c \tag{12}$$

where y_c is a sign function (0 or 1), take 1 if true class of sample i is equal to c, otherwise take 0; p_c is the predicted probability that the observed sample i belongs to category

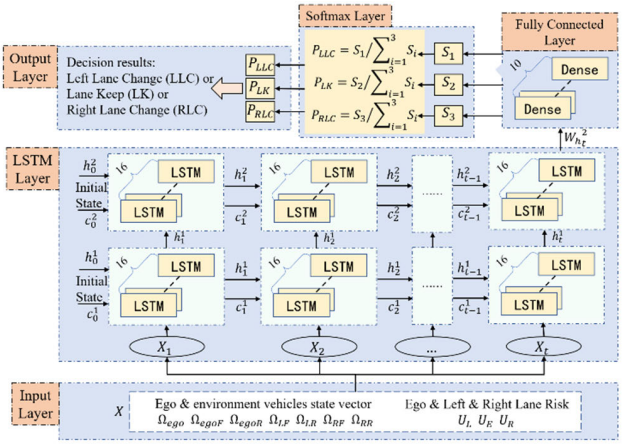

FIGURE 4. Lane change decision model based on LSTM.

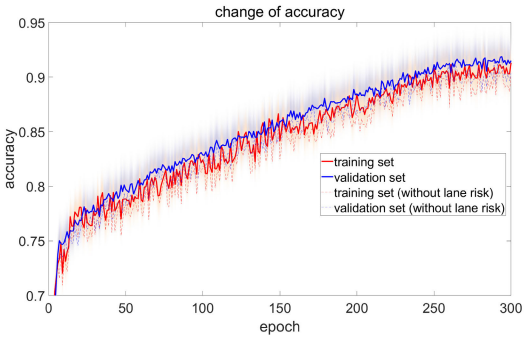

FIGURE 5. Change in accuracy rate of training process.

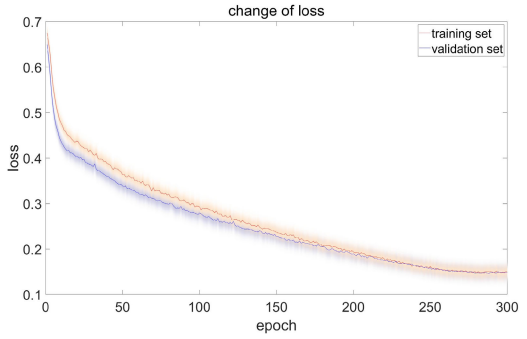

FIGURE 6. Change in loss of training process.

c; L is loss value. A decrease in cross-entropy loss means that the predicted value is close to the real. All inputs are normalized to [-1 1], and all data values and amplitudes that need to be adjusted are not large, so it is more suitable to use a small learning rate, set to 10^{-7}. The training epoch is set to 300, the batch size is set to 128, and a complete batch can be completed after 30 iterations.

Finally, the number of LSTM layers is 2 and the number of LSTM hidden layer is 16. The model structure is shown in Figure 4. The output of LSTM layer passes through a fully connected layer, then processed by the softmax classifier to obtain the value of the lane change decision:

$$P = [P_{LLC}, P_{LK}, P_{RLC}] \tag{13}$$

TABLE 2. Comparison results of different lane-change decision methods.

Methods	CA	LC-PR	LC-RR	LK-PR	LK-RR
Proposed method	92%	91%	87%	93%	95%
Proposed method (without lane risk)	90%	88%	86%	91%	92%
Bayes Network [26]	84%	84%		74%	
Support Vector Machine [27]	87%	87%		86%	

where P_{LLC}, P_{LK}, P_{RLC} is the probability of left lane change, lane keep, and right lane change respectively.

D. MODEL TRAINING AND VALIDATION

The changes in accuracy and loss function in the training process are shown in Figure 5 and Figure 6.

In order to illustrate that the introduction of lane risk can improve the accuracy of lane change decision, the model training proposed in this paper is divided into two parts: the training input layer of the first part is described in Fig.4, and the input layer of the other part of training removes the parameters representing lane risk. The result is shown in Table 2, where LC means lane change, LK means lane keeping, PR means precision rate, i.e., the real lane change decision sample in the results output by model, RR means recall rate, i.e., the proportion of lane change decision identified by the model. The final classification accuracy (CA) of the LSTM model proposed in this paper for driving decision is 92%, which is higher than 90% based on model without lane risk input, 84% based on Bayes network [26], and 87% based on support vector machine [27], as shown in Table 2.

III. TRAJECTORY PLANNING AND DYNAMIC CONTROL

In order to verify the reliability of the deep learning-based lane change decision model described in the previous section, this section performs trajectory planning and dynamic control on the samples which output as lane change decisions, in order to obtain good regulation and control results, so as to prove the correctness of the lane change model. Firstly, the lane change trajectory cluster is generated by setting a reasonable preview position interval, and the optimal trajectory is selected from trajectory cluster as reference. Then, simulation environment is set up to dynamically control the vehicle so that ego vehicle can track the reference trajectory. If simulated traffic flow is smooth, lane change decision made by the sample is justified.

A. LANE CHANGE TRAJECTORY PLANNING

The quintic polynomial can better imitate the lane change trajectory of human drivers for its smooth in acceleration, and various parameters such as curvature and lateral acceleration can meet the constraints in the lane change process, so it is often used for lane change trajectory planning. The relation between lateral displacement of vehicle time is

$$y = a_0 + a_1 t + a_2 t^2 + a_3 t^3 + a_4 t^4 + a_5 t^5 \tag{14}$$

where y is lateral offset of lane change. $a_5, a_4, a_3, a_2, a_1, a_0$ is coefficient of lane change trajectory; t is elapsed time since the start of lane changing. In the process of lane change trajectory planning, vehicle lateral velocity is the first derivative of lateral displacement with time, vehicle lateral acceleration is the second derivative of lateral displacement with time, and the change rate of lateral acceleration is the third derivative of vehicle lateral displacement with time.

$$\begin{cases} v_y = \dot{y}(t) = 5a_5t^4 + 4a_4t^3 + 3a_3t^2 + 2a_2t + a_1 \\ a_y = \ddot{y}(t) = 20a_5t^3 + 12a_4t^2 + 6a_3t + 2a_2 \\ \dot{a}_y = y(t) = 60a_5t^2 + 24a_4t + 6a_3 \end{cases} \tag{15}$$

where v_y is lateral velocity, a_y is lateral acceleration. The trajectory displacement, lateral velocity, acceleration, and rate of change expressed by the quintic polynomial are continuous and can satisfy kinematic constraints of vehicle. The specific shape of the polynomial is determined by coefficients of the polynomial $A = [a_0, a_1, a_2, a_3, a_4, a_5]^T$. Suppose at the initial moment of lane change $t = t_0$:

$$Y(t_0) = Y_0, v_y(t_0) = v_0, a_y(t_0) = a_0 \tag{16}$$

At the end moment of lane change t =t_{end}:

$$Y(t_{\text{end}}) = Y_{\text{end}}, v_y(t_{\text{end}}) = v_{\text{end}}, a_y(t_{\text{end}}) = a_{\text{end}} \tag{17}$$

Six polynomial equations can be constructed based on the state of vehicle at the initial and end moments:

$$\begin{cases} a_0 + a_1t_0 + a_2t_0^2 + a_3t_0^3 + a_4t_0^4 + a_5t_0^5 = Y_0 \\ a_0 + a_1t_{end} + a_2t_{end}^2 + a_3t_{end}^3 + a_4t_{end}^4 + \\ a_5t_{end}^5 = Y_{end} \\ a_1 + 2a_2t_0 + 3a_3t_0^2 + 4a_4t_0^3 + a_5t_0^4 = v_0 \\ a_1 + 2a_2t_{end} + 3a_3t_{end}^2 + 4a_4t_{end}^3 + a_5t_{end}^4 = v_{end} \\ 2a_2 + 6a_3t_0 + 12a_4t_0^2 + 20a_5t_0^3 = a_0 \\ 2a_2 + 6a_3t_{end} + 12a_4t_{end}^2 + 20a_5t_{end}^3 = a_{end} \end{cases} \tag{18}$$

where $a_5, a_4, a_3, a_2, a_1, a_0$ is the lane change trajectory coefficient; t_0 is start time of lane change, which is generally taken as 0; t_{end} is end time of lane change; Y_0, v_0, a_0 is the lateral position, lateral velocity, and lateral acceleration at the beginning of lane change, where the lateral position is generally taken as 0, and the latter two can be obtained by sensors; $Y_{end}, v_{end}, a_{end}$ is lateral position, lateral velocity, and lateral acceleration at the end of lane change. Vehicle lateral position is generally at the center line of target lane when the lane change finishes, and the lateral velocity and acceleration are 0. Under the premise of setting preview time, only the coefficient A = $[a_0, a_1, a_2, a_3, a_4, a_5]^T$ of the polynomial in the above multivariate equation is unknown. Substituting the initial time $t_0 = 0$ and the end time $t_{\text{end}} = t_{end}$ into the polynomial yields the coefficient

$$A = B^{-1}C \tag{19}$$

where

$$A = \begin{bmatrix} a_0 & a_1 & a_2 & a_3 & a_4 & a_5 \end{bmatrix}^T \tag{20}$$

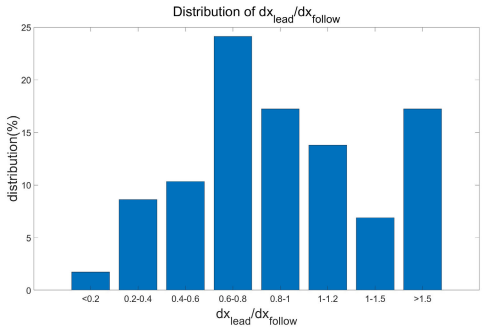

FIGURE 7. Proportional distribution of space with front & rear vehicle at end point of lane change.

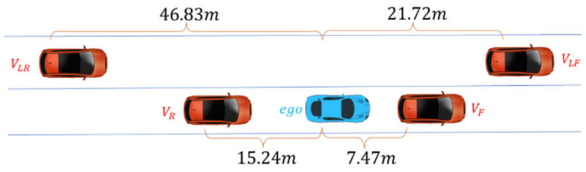

FIGURE 8. Relative position of lane change decision time.

$$B = \begin{bmatrix} 1 & 0 & 0 & 0 & 0 & 0 \\ 0 & 1 & 0 & 0 & 0 & 0 \\ 0 & 0 & 1 & 0 & 0 & 0 \\ 1 & t_{\text{end}} & (t_{\text{end}})^2 & (t_{\text{end}})^3 & (t_{\text{end}})^4 & (t_{\text{end}})^5 \\ 0 & 1 & 2t_{\text{end}} & 3(t_{\text{end}})^2 & 4(t_{\text{end}})^3 & 5(t_{\text{end}})^4 \\ 0 & 0 & 2 & 6t_{\text{end}} & 12(t_{\text{end}})^2 & 20(t_{\text{end}})^3 \end{bmatrix} \tag{21}$$

$$C = \begin{bmatrix} Y_0 & v_0 & a_0 & Y_{end} & v_{end} & a_{end} \end{bmatrix}^T \tag{22}$$

The vehicle state is the only certainty at the moment when lane change behavior is determined, so the quintic polynomial trajectory is only related to lane change time under specific driving conditions. When generating the ideal lane change trajectory, it is assumed that the vehicle is moving at a constant velocity in the longitudinal direction, so the lane change time can be calculated by $t_{\text{end}} = L/v_x$, L is the lane change preview displacement. Due to ego vehicle velocity is known, the lane change trajectory is determined by the preview distance, and the preview distance should be related to the relative distance of vehicles in front and rear of the target lane and their velocity. The ratio of distance from the front vehicle to the rear vehicle at the end of the lane change in the NGSIM dataset is shown in Figure 7.

When changing lanes, the driver has weak knowledge in intent and distance with rear vehicle, so the driver will first consider the distance from the front vehicle. After the end of lane change, the ratio of distance between the front and rear vehicles is the most between 0.6-0.8, followed by 0.8-1.0. Ratio greater than 1.5 is too far to give enough reference significance. Therefore, it can be considered that the ratio of distance from ego vehicle to front and rear vehicles after lane change is 0.8, which is the driver's priority lane change consideration.

Set a motion model in longitudinal direction and obtain the position relationship between ego vehicle obstacle vehicles in front and rear of target lane at the current moment. Set the complete time of lane change is t_{LC}, the longitudinal velocity of the lane change process is v_{ego}, and the longitudinal coordinate x of ego vehicle at the end of the lane change is

$$x = v_{ego} * t_{LC} \tag{23}$$

The longitudinal coordinates of the front and rear obstacle vehicles after lane change is

$$\begin{cases} x_{tar_F} = x_{0_F} + v_{tar_F} * t_{LC} \\ x_{tar_R} = x_{0_R} + v_{tar_R} * t_{LC} \end{cases} \tag{24}$$

where x_{tar_F} and x_{tar_R} are the longitudinal coordinates of front and rear vehicle at the end of the lane change, x_{0_F} and x_{0_R} are the coordinates of front and rear vehicle at the beginning of lane change, v_{tar_F} and v_{tar_R} are the longitudinal velocity of front and rear vehicle at beginning of the lane change, respectively. The ratio of distance to front and rear vehicle at the end of the lane change is 0.8.

$$\frac{x - x_{tar_R}}{x_{tar_F} - x} = 0.8 \tag{25}$$

When lane change has finished, the change time to meet the ideal distance between the front and rear vehicle is t_{LC}

$$t_{LC} = \frac{x_{0_R} + 0.8x_{0_F}}{1.8v_{ego} - v_{t_{tar_R}} - 0.8v_{tar_F}} \tag{26}$$

According to the conclusion of [25], the time distribution of the lane change execution stage is between 1.5-13.9s, and the average value is 6.97 s. This paper limits the lane change time to 5-10s, if the calculated lane change time is less than 5s, take 5s, take 10s if it is greater than 10s, and if the calculation conditions are not met, take the average lane change time 7s. the preview distance dis_{LC} can be obtained with lane change time t_{LC} by

$$dis_{LC} = v_{ego} * t_{LC} \tag{27}$$

Set 5 and 4 alternate preview points at intervals of 2 meters in front and rear of the preview distance, and calculate the trajectory cluster formed by the ten preview points.

B. SELECTION AND SIMULATION OF LANE CHANGE TRAJECTORY

Under the premise that the lateral distance of the lane change is fixed, the long lane change time will bring a small yaw rate and angular acceleration, so as to increase comfort. However, too long time of lane change can affect the flow of traffic. Therefore, the selection of lane change trajectory should consider both traffic efficiency and drive comfort, expressed by cost function

$$J = w_1 J_{eff} + w_2 J_{com} \tag{28}$$

$$\begin{cases} w_1 + w_2 = 1 \\ 0 < w_1 < 1 \\ 0 < w_2 < 1 \end{cases} \tag{29}$$

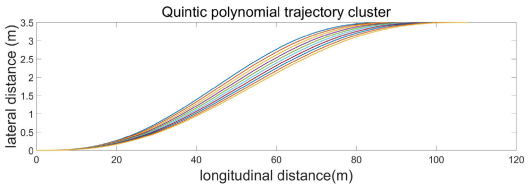

FIGURE 9. Lane change trajectory cluster.

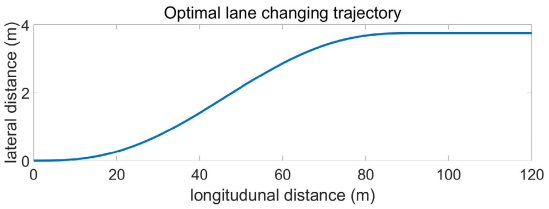

FIGURE 10. Selected optimal lane change trajectory.

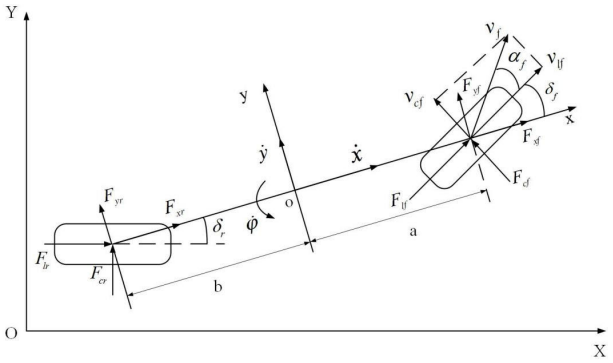

FIGURE 11. Three-degree-freedom vehicle dynamics model based on ground coordinate system.

where J_{eff} characterizes lane change efficiency, J_{com} characterizes driving comfort, w_1 and w_2 represent the weight of lane change efficiency and comfort, respectively. In this paper, traffic efficiency is characterized by the ratio of the longitudinal distance x_{fin} to the maximum longitudinal distance x_{max} of lane change, the longer the continuous distance of the lane change, the lower traffic efficiency.

$$J_{eff} = \frac{x_{fin}}{x_{max}} \tag{30}$$

The ratio of the average lateral acceleration a_{avg} to its maximum $a_{avg_{limit}}$ during lane change and the ratio of the maximum lateral acceleration a_{max} to its maximum $a_{max_{limit}}$ are used as evaluation criteria for drive comfort.

$$J_{com} = \frac{a_{avg}}{a_{avg_{limit}}} + \frac{a_{max}}{a_{max_{limit}}} \tag{31}$$

Then cost function J is expressed as

$$J = w_1 \frac{x_{fin}}{x_{max}} + w_2 \left(\frac{a_{avg}}{a_{avg_{limit}}} + \frac{a_{max}}{a_{max_{limit}}} \right) \tag{32}$$

In trajectory cluster, the trajectory with smallest evaluation function is screened out as the final reference trajectory.

Based on the above method for simulation, a piece of vehicle data is selected from NGSIM data set, and surrounding environment of ego vehicle is shown in Figure 8. Select $w_1 = w_2 = 0.5$, and ego vehicle velocity is $v_{ego} = 12.2\text{m/s}$. The velocity of front obstacle vehicle in current lane is $v_{front} = 10.11\text{m/s}$. The velocity of rear obstacle vehicle in current lane is $v_{rear} = 12.18\text{m/s}$. The velocity of right front obstacle vehicle is $v_{rightfront} = 13.72\text{m/s}$. The velocity of right rear vehicle is $v_{rightrear} = 14.03\text{m/s}$. The calculated lane change time and longitudinal distance are: $t_{LC} = 8.2\text{s}$; $dis_{LC} = 100\text{m}$, the trajectory cluster generated according to the driving conditions at the time of lane change decision is shown in Figure 9. The lateral velocity and acceleration of the above trajectory cluster are calculated. Based on the evaluation function, all trajectories in the trajectory cluster are quantitatively evaluated, and the lane change trajectory with the smallest evaluation function is the one with the lane change distance equal to 94m, and preview time is 7.7s, as shown in Figure 10.

C. MPC-BASED DYNAMICS CONTROL

After lane change trajectory planning, a reasonable trajectory tracking method needs to be designed so that ego vehicle can follow the desired trajectory quickly and smoothly. Firstly, the vehicle dynamics model is built, and then the trajectory tracking controller is designed based on MPC. The used three-degree-freedom dynamic model is shown in Figure 11, where OXY is the ground coordinate system, oxy is the vehicle coordinate system, the o point is at the position of vehicle center of mass, the x-axis points to the longitudinal axis of vehicle, and the y axis is perpendicular to the x-axis to the left.

From geometric relations we can get

$$\dot{X} = \dot{x}\,cos\varphi - \dot{y}\,sin\varphi \tag{33}$$

$$\dot{Y} = \dot{x}\,sin\varphi + \dot{y}\,cos\varphi \tag{34}$$

Under the ground coordinate system, X is longitudinal displacement, $\dot{X}$ is longitudinal velocity, Y is lateral displacement, $\dot{Y}$ is lateral velocity. Under vehicle coordinate system, φ is yaw angle, $\dot{x}$ is longitudinal velocity, $\dot{y}$ is lateral velocity.

The force balance equation for the vehicle's translational motion in the x-axis and y-axis, and rotational motion around the z-axis is

$$\begin{cases} m\ddot{x} = m\dot{y}\dot{\varphi} + 2F_{xf} + 2F_{xr} \\ m\ddot{y} = -m\dot{x}\dot{\varphi} + 2F_{yf} + 2F_{yr} \\ I_z\ddot{\varphi} = 2aF_{yf} - 2bF_{yr} \end{cases} \tag{35}$$

where $\ddot{x}$ is longitudinal acceleration; $\dot{\varphi}$ is vehicle yaw rate; F_{xf}, F_{xr} is force in the x direction of front and rear wheels; $\ddot{y}$ is longitudinal acceleration; F_{yf}, F_{yr} is force in the y direction of front and rear wheels; I_z is vehicle inertia around the z-axis; $\ddot{\varphi}$ is vehicle yaw angle acceleration; a, b are front and rear wheelbase.

Longitudinal and lateral forces of the wheels are calculated as follows:

$$\begin{cases} F_{xf} = C_{lf}\,s_f \\ F_{xr} = C_{lr}\,s_r \\ F_{yf} = C_{cf}\left(\delta_f - \dfrac{\dot{y} + a\dot{\varphi}}{\dot{x}}\right) \\ F_{yr} = C_{cr}\dfrac{b\dot{\varphi} - \dot{y}}{\dot{x}} \end{cases} \tag{36}$$

where C_{lf}, C_{lr} are longitudinal stiffness of front and rear wheels, C_{cf}, C_{cr} are lateral stiffness of front and rear wheels, s_f, s_r are slip rate of the front and rear wheels, a, b are front and rear wheelbase of the vehicle, δ_f is front wheel angle. Then the vehicle dynamics model can be expressed as

$$\begin{cases} m\ddot{x} = m\dot{y}\dot{\varphi} + 2\left[C_{lf}\,s_f + C_{cf}\left(\delta_f - \dfrac{\dot{y} + a\dot{\varphi}}{\dot{x}}\right)\delta_f + C_{lr}\,s_r\right] \\ \dot{X} = \dot{x}\,cos\varphi - \dot{y}\,sin\varphi \\ m\ddot{y} = -m\dot{x}\dot{\varphi} + 2\left[C_{cf}\left(\delta_f - \dfrac{\dot{y} + a\dot{\varphi}}{\dot{x}}\right) + C_{cr}\dfrac{b\dot{\varphi} - \dot{y}}{\dot{x}}\right] \\ \dot{Y} = \dot{x}\,sin\varphi + \dot{y}\,cos\varphi \\ I_z\ddot{\varphi} = 2\left[aC_{cf}\left(\delta_f - \dfrac{\dot{y} + a\dot{\varphi}}{\dot{x}}\right) - bC_{cr}\dfrac{b\dot{\varphi} - \dot{y}}{\dot{x}}\right] \end{cases} \tag{37}$$

In this system, a set of state variables can be written as $\xi_{dyn} = [\dot{y}, \dot{x}, \varphi, \dot{\varphi}, Y, X]^T$, a set of control variables can be written as $u_{dyn} = [\delta_f]$. The linearization process yields a time-varying equation as

$$\dot{\xi}_{dyn} = A_{dyn}(t)\,\xi_{dyn}(t) + B_{dyn}(t)\,u_{dyn}(t) \tag{38}$$

where (39) and (40), as shown at the bottom of the next page.

Discretization as

$$\xi_{dyn}(k+1) = A_{dyn}(k)\,\xi_{dyn}(k) + B_{dyn}(k)\,u_{dyn}(k) \tag{41}$$

where $A_{dyn}(k) = I + TA_{dyn}(t)$, $B_{dyn}(k) = TB_{dyn}(t)$, k is the moment at which the current step is located, T is sampling period, and I is unit matrix.

The constraint on the control variables is

$$\begin{cases} -25^\circ \le \delta \le 25^\circ \\ -0.47^\circ \le \Delta\delta \le 0.47^\circ \end{cases} \tag{42}$$

The ultimate goal of trajectory tracking is to ensure that the vehicle follows the desired trajectory quickly and smoothly, so the tracking offset is considered in the objective function. The control increment into the objective function is written as follows:

$$\begin{aligned} &\min_{\Delta u} J\left(\xi_{dyn}(t), u_{dyn}(t-1), \Delta u(k)\right) \\ &= \sum_{i=1}^{N_p} \left\| \eta_{dyn}(t+i\,|\,t) - \eta_{dyn,ref}(t+i\,|\,t) \right\|_Q^2 \\ &\quad + \sum_{i=1}^{N_c-1} \left\| \Delta u(k+i) \right\|_R^2 \end{aligned} \tag{43}$$

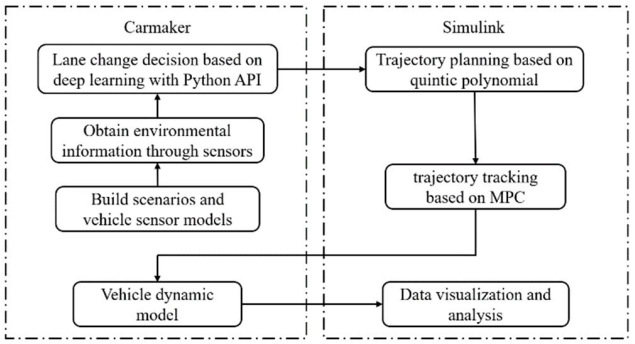

FIGURE 12. Illustration of the simulation process.

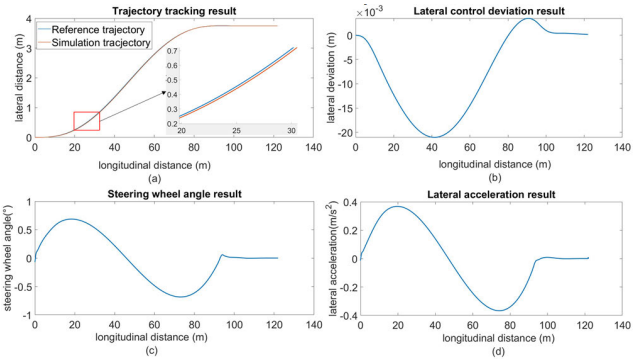

FIGURE 13. Real driving condition simulation (a). trajectory tracking (b). lateral control deviation (c). steering wheel angel (d). lateral acceleration.

$$s.t.\begin{cases} u_{min} \le u\left(k+i\right) \le u_{max} \\ \Delta u_{min} \le \Delta u\left(k+i\right) \le \Delta u_{max} \\ y_{min} \le y \le y_{max} \end{cases} \tag{44}$$

where $\Delta u\left(k\right)$ is the increment of control variable in the k-th period, $\eta_{dyn} = [Y, \varphi]$ is predicted value (lateral offset and yaw angle) output in control process, $\eta_{dyn,ref} = \left[Y_{ref}, \varphi_{ref}\right]$ is reference values for η_{dyn}, $(t+i\,|\,t)$ means to predict information at time $t+1$ based on information at the sampling time t, $i = 1, 2, 3, \ldots, N_p$. N_p, N_c is predict horizon and control horizon. Q, R represents weight matrix of output variable and control variable increment, u_{min}, u_{max} is lower and upper limits of the control variable, $\Delta u_{min}, \Delta u_{max}$ is lower and upper limits of the control variable increment.

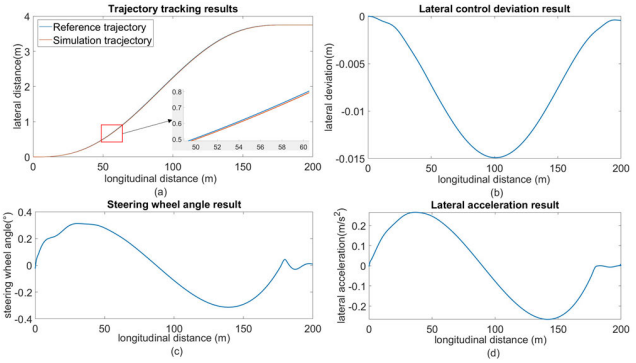

FIGURE 14. Highway driving condition simulation (a). trajectory tracking (b). lateral control deviation (c). steering wheel angel (d). lateral acceleration.

The above equation is solved in every period to obtain a series of control variable increments:

$$\Delta U^*_{dyn,t} = \left[\Delta u^*_{dyn,t}, \Delta u^*_{dyn,t+1}, \cdots, \Delta u^*_{dyn,t+N_c-1}\right]^T \tag{45}$$

The first element of the solved result acts on the controlled system:

$$u_{dyn}\left(t\right) = u_{dyn}\left(t-1\right) + \Delta u^*_{dyn,t} \tag{46}$$

The above process calculations are carried out in every control period to complete the target trajectory tracking of ego vehicle.

IV. SIMULATION RESULTS

In the Carmaker platform, select ego vehicle model and corresponding sensor model to establish a random traffic flow. Next read the state of obstacle vehicles around ego vehicle from the environment information. Then control the vehicle model in Carmaker through the autonomous lane change decision, trajectory planning, and tracking controller established in Simulink. The simulation logic is shown in Figure 12.

First, the real driving condition described in Section III-A is simulated, under which the velocity of ego vehicle is 12.2 m/s, and the preview time is calculated as 7.7 s and preview distance is 94 m according to the driving condition at

$$A_{dyn}\left(t\right) = \left.\frac{\partial f_{dyn}}{\partial \xi_{dyn}}\right|_{\hat{\xi}_t, u_t} = \begin{bmatrix} -\frac{2(C_{cf}+C_{cr})}{m\dot{x}_t} & \frac{\partial f_{\dot{y}}}{\partial \dot{x}} & 0 & -\dot{x}_t + \frac{2(bC_{cr}-aC_{cf})}{m\dot{x}_t} & 0 & 0 \\ \dot{\varphi} - \frac{2C_{cf}\delta_{f,t-1}}{m\dot{x}_t} & \frac{\partial f_{\dot{x}}}{\partial \dot{x}} & 0 & \dot{y}_t - \frac{2aC_{cf}\delta_{f,t-1}}{m\dot{x}_t} & 0 & 0 \\ 0 & 0 & 0 & 1 & 0 & 0 \\ \frac{2(bC_{cr}-aC_{cf})}{I_z\dot{x}_t} & \frac{\partial f_{\dot{\varphi}}}{\partial \dot{x}} & 0 & -\frac{2(a^2C_{cf}+b^2C_{cr})}{I_z\dot{x}_t} & 0 & 0 \\ cos\left(\varphi_t\right) & sin\left(\varphi_t\right) & \dot{x}_t\, cos\left(\varphi_t\right) - \dot{y}_t\, sin\left(\varphi_t\right) & 0 & 0 & 0 \\ -sin\left(\varphi_t\right) & cos\left(\varphi_t\right) & -\dot{y}_t\, cos\left(\varphi_t\right) - \dot{x}_t\, sin\left(\varphi_t\right) & 0 & 0 & 0 \end{bmatrix} \tag{39}$$

$$B_{dyn}\left(t\right) = \left.\frac{\partial f_{dyn}}{\partial u_{dyn}}\right|_{\hat{\xi}_t, u_t} = \left[\frac{2C_{cf}}{m}, \frac{2C_{cf}\left(2\delta_{f,t-1} - \frac{\dot{y}_t + a\dot{\varphi}_t}{\dot{x}_t}\right)}{m}, 0, \frac{2aC_{cf}}{I_z}, 0, 0\right] \tag{40}$$

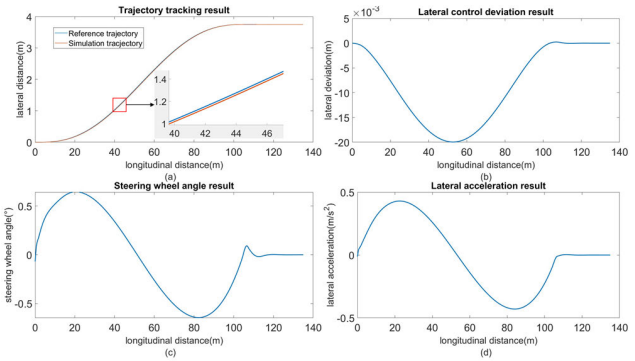

FIGURE 15. Urban driving condition simulation (a). trajectory tracking (b). lateral control deviation (c). steering wheel angel (d). lateral acceleration.

the beginning of lane change, and the simulation results are shown in Figure 13.

Highway condition simulation, ego vehicle velocity is: $v_{ego} = 20\text{m/s}$. Velocity of the vehicle in front of current lane is: $v_{front} = 18\text{m/s}$. Velocity of the vehicle in front of target lane is: $v_{rightfront} = 23\text{m/s}$, front distance is 40 m. Velocity of rear vehicle in target lane is: $v_{rightrear} = 21\text{m/s}$, rear distance is -40 m. Lane change decision is made based on the low speed of the vehicle in front and the condition of adjacent lane. At the beginning of lane change, trajectory planning is carried out, and lane change time and longitudinal distance are calculated as: $t_{LC} = 9\text{s}$; $dis_{LC} = 180\text{m}$. The simulation results are shown in Figure 14.

Urban condition simulation is similar with highway simulation, here we set $v_{ego} = 15\text{m/s}$, $v_{front} = 10\text{m/s}$, front distance is 40 m, $v_{rightrear} = 15\text{m/s}$, rear distance is -30m. Then lane change time and longitudinal distance are calculated as: $t_{LC} = 7\text{s}$, $dis_{LC} = 105\text{m}$. The simulation results are shown in Figure 15.

The analysis of the simulation results shows that the model can track the planning path with stable changes of the control variable and state variable. The simulation results show that the system can adapt to various velocity conditions to complete the lane change task.

V. CONCLUSION

Through the analysis of lane change data, this paper links the abstract free lane change decision with the physical characteristics of vehicles, and extracts factors affecting driver's decision in free lane change, including lane risk and trajectory information of ego vehicle and environmental obstacle vehicles. While calculating the lane value, this paper considers the size information of obstacle vehicles, which increases the input dimension, and is an improvement on the past work. Then, a data-driven method is used to obtain the training sample set and build a deep learning model, and the model training results proves that the correct rate of the selected LSTM-based lane change decision model is more than 92%, which can adapt to most driving conditions. Next, a lane change trajectory cluster generation and evaluation method based on preview time is proposed to select the optimal lane change trajectory, and a lane change trajectory planning method is obtained. The three-degree-freedom dynamic vehicle model is analyzed and linearized, and a trajectory tracking model based on MPC method is designed. The FLC decision making and proportional distribution of front and rear space at end point of lane change based on real driving data, and the trajectory planner is based on quintic polynomial, which can provide human-like elements for lane change process. Finally, the Carmaker/Simulink co-simulation platform is used to design different driving conditions to simulate the lane changing system, and the results show that the deep learning decision and autonomous lane change method proposed in this paper can adapt to different driving conditions to complete the lane change task.

The next step of this research can try to expand the amount of data of the deep learning model with a richer dataset, add more considerations such as driver's t personalized style to the model input, and further verify the real vehicle to improve the randomness of the experimental scene.

REFERENCES

[1] P. G. Gipps, "A model for the structure of lane-changing decisions," *Transp. Res. B, Methodol.*, vol. 20, no. 5, pp. 403–414, Oct. 1986.

[2] Y. Li, R. Gu, J. Lee, M. Yang, Q. Chen, and Y. Zhang, "The dynamic trade-off between safety and efficiency in discretionary lane-changing behavior: A random parameters logit approach with heterogeneity in means and variances," *Accident Anal. Prevention*, vol. 153, Apr. 2021, Art. no. 106036.

[3] Y. Jia, D. Qu, H. Song, T. Wang, and Z. Zhao, "Car-following characteristics and model of connected autonomous vehicles based on safe potential field," *Phys. A, Stat. Mech. Appl.*, vol. 586, Jan. 2022, Art. no. 126502.

[4] X. Long, L. Zhang, S. Liu, and J. Wang, "Research on decision-making behavior of discretionary lane-changing based on cumulative prospect theory," *J. Adv. Transp.*, vol. 2020, Jan. 2020, Art. no. 1291342.

[5] Q. Zeng, G. Wu, and L. Mao, "A support vector machine-based truck discretionary lane changing decision model," in *Proc. 20th Int. Conf. Adv. Robot. (ICAR)*, Dec. 2021, pp. 435–440.

[6] Y. Feng and X. Yan, "Support vector machine based lane-changing behavior recognition and lateral trajectory prediction," *Comput. Intell. Neurosci.*, vol. 2022, May 2022, Art. no. 3632333.

[7] O. Sharma, N. C. Sahoo, and N. B. Puhan, "Highway lane-changing prediction using a hierarchical software architecture based on support vector machine and continuous hidden Markov model," *Int. J. Intell. Transp. Syst. Res.*, vol. 20, no. 2, pp. 519–539, Aug. 2022.

[8] M. Liu and J. Shi, "A cellular automata traffic flow model combined with a BP neural network based microscopic lane changing decision model," *J. Intell. Transp. Syst.*, vol. 23, no. 4, pp. 309–318, Jul. 2019.

[9] B. Wang, Z. Li, S. Wang, M. Li, and A. Ji, "Modeling bounded rationality in discretionary lane change with the quantal response equilibrium of game theory," *Transp. Res. B, Methodol.*, vol. 164, pp. 145–161, Oct. 2022.

[10] J. Guo and I. Harmati, "Lane-changing decision modelling in congested traffic with a game theory-based decomposition algorithm," *Eng. Appl. Artif. Intell.*, vol. 107, Jan. 2022, Art. no. 104530.

[11] Y. Jiang, B. Zhu, and X. Zhao, "Modeling of traffic vehicle interaction for autonomous vehicle testing," *Automot. Eng.*, vol. 44, no. 12, pp. 1825–1833, 2022.

[12] J. Lee and J. W. Choi, "May I cut into your lane? A policy network to learn interactive lane change behavior for autonomous driving," in *Proc. IEEE Intell. Transp. Syst. Conf. (ITSC)*, Auckland, New Zealand, Oct. 2019, pp. 4342–4347.

[13] S. Mozaffari, E. Arnold, M. Dianati, and S. Fallah, "Early lane change prediction for automated driving systems using multi-task attention-based convolutional neural networks," *IEEE Trans. Intell. Vehicles*, vol. 7, no. 3, pp. 758–770, Sep. 2022.

[14] D.-F. Xie, Z.-Z. Fang, B. Jia, and Z. He, "A data-driven lane-changing model based on deep learning," *Transp. Res. C, Emerg. Technol.*, vol. 106, pp. 41–60, Sep. 2019.
[15] D. Li and A. Liu, "Personalized lane change decision algorithm using deep reinforcement learning approach," *Appl. Intell.*, vol. 53, pp. 13192–13205, Oct. 2022.
[16] X. Xu, L. Zuo, X. Li, L. Qian, J. Ren, and Z. Sun, "A reinforcement learning approach to autonomous decision making of intelligent vehicles on highways," *IEEE Trans. Syst., Man, Cybern., Syst.*, vol. 50, no. 10, pp. 3884–3897, Oct. 2020.
[17] R. Zhang, Z. Zhang, Z. Guan, Y. Li, and Z. Li, "Autonomous lane changing control for intelligent vehicles," *Cluster Comput.*, vol. 22, no. S4, pp. 8657–8667, Jul. 2019.
[18] R. van Hoek, J. Ploeg, and H. Nijmeijer, "Cooperative driving of automated vehicles using B-splines for trajectory planning," *IEEE Trans. Intell. Vehicles*, vol. 6, no. 3, pp. 594–604, Sep. 2021.
[19] W. Lim, S. Lee, M. Sunwoo, and K. Jo, "Hierarchical trajectory planning of an autonomous car based on the integration of a sampling and an optimization method," *IEEE Trans. Intell. Transp. Syst.*, vol. 19, no. 2, pp. 613–626, Feb. 2018.
[20] M. Boryga, P. Kołodziej, and K. Gołacki, "The use of asymmetric polynomial profiles for planning a smooth trajectory," *Appl. Sci.*, vol. 12, no. 23, p. 12284, Nov. 2022.
[21] Y. Li, X. N. Wang, S. J. Li, and J. Zhu, "LQR based trajectory tracking control for forked AGV," in *Proc. 3rd Int. Conf. Mech., Contro, Electron. Inf. (ICMCEI)*, 2014, pp. 447–451.
[22] J. Liu, H. Weng, Y. Hu, H. Huang, and Y. Song, "Driver-in-the-loop handling stability control of 4WID-EV," *Int. J. Automot. Technol.*, vol. 23, no. 2, pp. 345–356, Apr. 2022.
[23] Y. Nie, M. Zhang, and X. Zhang, "Trajectory tracking control of intelligent electric vehicles based on the adaptive spiral sliding mode," *Appl. Sci.*, vol. 11, no. 24, p. 11739, Dec. 2021.
[24] A. Doshi, B. Morris, and M. Trivedi, "On-road prediction of driver's intent with multimodal sensory cues," *IEEE Pervasive Comput.*, vol. 10, no. 3, pp. 22–34, Jul. 2011.
[25] S. Zhang, H. Peng, S. Nageshrao, and E. Tseng, "Discretionary lane change decision making using reinforcement learning with model-based exploration," in *Proc. 18th IEEE Int. Conf. Mach. Learn. Appl. (ICMLA)*, Dec. 2019, pp. 844–850.
[26] J. Q. Wang, R. Chai, and N. Cao, "Modeling highway lane changing using Bayesian networks," in *Proc. 3rd Int. Conf. Civil Eng. Transp. (ICCET)*, 2013, pp. 1143–1147.
[27] Y. Liu, X. Wang, L. Li, S. Cheng, and Z. Chen, "A novel lane change decision-making model of autonomous vehicle based on support vector machine," *IEEE Access*, vol. 7, pp. 26543–26550, 2019.
[28] Z.-Q. Liu, M.-C. Peng, and Y.-C. Sun, "Estimation of driver lane change intention based on the LSTM and Dempster–Shafer evidence theory," *J. Adv. Transp.*, vol. 2021, Jan. 2021, Art. no. 8858902.
[29] Q. Shi and H. Zhang, "An improved learning-based LSTM approach for lane change intention prediction subject to imbalanced data," *Transp. Res. C, Emerg. Technol.*, vol. 133, Dec. 2021, Art. no. 103414.
[30] D. Chu, H. Li, C. Zhao, and T. Zhou, "Trajectory tracking of autonomous vehicle based on model predictive control with PID feedback," *IEEE Trans. Intell. Transp. Syst.*, vol. 24, no. 2, pp. 2239–2250, Feb. 2023.
[31] Y. Xu, W. Tang, B. Chen, L. Qiu, and R. Yang, "A model predictive control with preview-follower theory algorithm for trajectory tracking control in autonomous vehicles," *Symmetry*, vol. 13, no. 3, p. 381, Feb. 2021.
[32] N. Zhu and Z. Gao, "Research on personalized lane change triggering based on traffic risk assessment," *Automot. Eng.*, vol. 43, no. 9, pp. 1314–1321, 2021.

LIANG CHU (Member, IEEE) was born in 1967. He received the B.S., M.S., and Ph.D. degrees in vehicle engineering from Jilin University, Changchun, China.

He is currently a Professor and a Ph.D. Supervisor with the College of Automotive Engineering, Jilin University. His research interests include the driving and braking theory and control technology for vehicles. He is a member of the Teaching Committee of Mechatronics Discipline Committee of the China Machinery Industry Education Association.

JIAWEI WANG was born in 1996. He received the B.S. degree in automotive engineering from Jilin University, Changchun, China, in 2018, where he is currently pursuing the integrated master's and Ph.D. degree in automotive engineering.

His research interests include the development of intelligent driving planning and control algorithms, as well as autonomous vehicle testing methods.

ZHUO CAO was born in 1998. He received the B.S. and M.S. degrees in automotive engineering from Jilin University, Changchun, China, in 2020 and 2023, respectively.

His research interests include decision making and planning for autonomous vehicle and the dynamics and control of vehicles.

YAO ZHANG was born in 1994. He received the B.S. and M.S. degrees in automotive engineering from Jilin University, Changchun, China, in 2015 and 2018, respectively, where he is currently pursuing the Ph.D. degree.

His research interests include in-wheel motor vehicle control and automated driving, particularly trajectory planning and control for lane-changing scenario.

CHONG GUO received the B.S. degree in electronical information science and technology and the Ph.D. degree in vehicle engineering from Jilin University, Changchun, China, in 2009 and 2016, respectively.

He is currently an Associate Professor with the College of Automotive Engineering, Jilin University. His research interests include decision making and planning for autonomous vehicle, and the dynamics and control of vehicles.